JOURNAL OF MATERIALS SCIENCE **40** (2005) 285–293

The morphology and topography of polymer surfaces and interfaces exposed by ultra-low-angle microtomy

S. J. HINDER
The Surface Analysis Laboratory, School of Engineering, University of Surrey, Guildford, Surrey GU2 7XH, UK
E-mail: s.hinder@surrey.ac.uk

C. LOWE, J. T. MAXTED
Becker Industrial Coatings Ltd., Goodlass Road, Speke, Liverpool L24 9HJ, UK

J. F. WATTS
The Surface Analysis Laboratory, School of Engineering, University of Surrey, Guildford, Surrey GU2 7XH, UK

The ultra-low-angle microtomy (ULAM) technique has been developed to impart a cross-sectional, ultra-low-angle taper through polymeric materials such as coatings and paints. ULAM employs a conventional rotary microtome in combination with high-precision, angled sectioning blocks to fabricate the ultra-low-angle tapers. Subsequent investigation of the tapers produced by ULAM may be used in conjunction with X-ray photoelectron spectroscopy (XPS) or time-of-flight secondary ion mass spectrometry (ToF-SIMS), for compositional depth profiling or 'buried' interface analysis. Variation in the selection of the ULAM taper angle and/or the analysis interval size employed enables depth resolution at the nanometre or micrometre scales to be achieved.

In the work described here scanning electron microscopy (SEM) and atomic force microscopy (AFM) have been employed to investigate the morphology and topography of the surfaces resulting from the ULAM tapering process. It is demonstrated that a correctly mounted polymeric sample, sectioned with a sharp microtome knife, displays little perturbation of the resulting polymeric surface after ULAM processing. Additionally, SEM analysis of the interface region between a poly(vinylidene fluoride) (PVdF) topcoat and polyurethane (PU) primer exposed by ULAM processing reveals that the interface region between the two coatings possesses a well-defined boundary. No evidence of polymeric smearing across the interface is observed. XPS compositional depth profiling across a 'buried' PVdF/PU interface, exposed by ULAM processing, is employed to demonstrate the utility of the ULAM technique.

1. Introduction

The desire to probe below the surface of a sample either to investigate changes of composition with depth or to access interfaces 'buried' below overlying material is a common challenge encountered by the materials scientist or engineer. Surface specific depth profiling techniques such as angle resolved X-ray photoelectron spectroscopy can be employed to produce composition depth profiles but are usually limited to the topmost 5 nm or so of the sample material [1]. Alternatively techniques such as Rutherford backscattering spectroscopy can probe sample depths approaching 1 μm [2]. However, whilst sputter depth profiling using noble gas or liquid metal ions is the most widely employed technique to produce compositional depth profiles the technique is typically limited to a few microns in materials which sputter in a predictable and non-degrading manner. Polymers are not amenable to this means of processing. If it is necessary to probe deep below the surface and yet retain depth resolution, alternative methods must be sought.

A different approach to the direct analysis techniques described above is to employ an instrument such as a microtome to produce cross-sections through a material by means of a series of serial sections for subsequent analysis. Girois *et al.* have employed microtomed sections 40 μm thick to investigate the photooxidation of isotactic polypropylene [3] whilst Anton-Prinet *et al.* used 20 μm thick serial sections to produce degradation thickness profiles of poly(vinyl chloride) that had undergone photoageing [4]. Although the microtoming technique has been applied to a wide range of polymeric materials, the depth resolution achievable is governed by the practicalities of cutting and handling the material

sections produced, typically a resolution of no better than 6–10 μm can be achieved when sectioning polymeric samples [5].

The use of *ex-situ* mechanical techniques that remove material from a sample in a precise manner and that produce specimens possessing a well-defined geometry have a well documented history. Two such techniques that have been widely reported are those of ball cratering and angle lapping. In the ball cratering procedure a steel ball bearing coated in a diamond paste is rotated against a specimen so as to produce a shallow crater at the sample surface. The specimen must then be introduced to a spectrometer and a brief ion etch of the tapered surface employed to remove any contaminants from the ball cratering procedure. Linescan or point analysis by Auger electron spectroscopy along the crater wall then yields a compositional depth profile of the sample material [6, 7]. The angle lapping technique [8] was the forerunner of ball cratering, in that sample material is removed from a specimen by abrading and polishing. In the angle lapping procedure the specimen is polished at an angle of $<3^\circ$ so as to produce a shallow taper through the material of interest. As with ball cratering the lapped specimen must be introduced to a spectrometer and a brief ion etch of the tapered surface performed to remove any contaminants from the angle lapping process. A linescan or point analysis along the tapered surface of the sample yields a compositional depth profile that can be readily converted to a depth of analysis from the starting point.

Ball cratering and angle lapping have typically been used to investigate metallic, alloyed and inorganic material systems. Walls *et al.* employed ball cratering to examine Zn coatings on steel and nitrocarburised steel surfaces [6, 7] whilst Hintermann and Chollet used the technique on TiN coatings on steel [9]. Tarng and Fisher have employed angle lapping to investigate polysilicon and lead-boro-aluminosilicate coatings on SiO_2/Si substrate [8] while Lea and Seah used Ag on Fe to evaluate the lapping procedure [10]. When techniques such as ball cratering and angle lapping, which rely upon an abrading or polishing mechanism to remove sample material, are applied to organic systems such as polymeric materials the resulting crater or taper surfaces generally suffer from smearing of the polymeric material leading to a loss of resolution and the possibility that the abrading/polishing mechanism induces physical or chemical change and/or artefacts. However, although Cohen and Castle have demonstrated that ball cratering can be employed to investigate polymer-steel interfaces, this analysis required precise control of the sample temperature by means of a cryo-stage [11].

The ULAM technique is a logical extension of the angle lapping procedure, however, ULAM provides the additional benefit in that it can be applied to a range of materials that would undergo smearing or deformation if processed by angle lapping. In the studies reported here the ULAM technique is described in detail and Scanning Electron Microscopy (SEM) and Atomic Force Microscopy (AFM) are used to investigate the morphology and topography respectively of ULAM fabricated tapered surfaces that pass through a model multilayer PVdF topcoat and PU primer coating system interface. Additionally, the applicability of ULAM tapers to the analysis of polymeric coatings and paints is demonstrated by the use of X-ray photoelectron spectroscopy (XPS) compositional depth profiling across a PVdF/PU interface buried over 20 μm below the PVdF topcoat surface.

2. Experimental

2.1. Materials and methods

The PVdF topcoat and PU primer coating samples on an Al substrate used as a model, multilayer, coating system were produced by Becker Industrial Coatings Ltd. The polymeric topcoat was a PVdF based commercial formulation in which mainly blue and white pigments were incorporated. The colour aided identification of the interfacial layer. The underlying primer coating is a PU based commercial formulation which incorporates a yellow pigment. Samples were provided as cured coatings on Al panels ($\sim$60 $\times$ 100 mm). In addition a model powder coating system comprising the commercially available powder coating RILSAN B® (polyamide 11) (Atofina, Serquigny, France) to which 3-aminopropyl triethoxysilane (APS) (Sigma-Aldrich, Poole, UK) had been added was employed. Liquid APS was added to RILSAN B powder stock and mixed in a rotary mixing chamber for 100 s prior to application to a grit blasted steel panel (10,000 mm^2 $\times$ 1 mm) via an electrostatic gun. Once applied the coating was heated to 210°C for 10 min, the resulting coating was typically 80 to 120 μm thick [12]. Thus polymeric specimens that were either thermosetting (polyurethane) or thermoplastic (polyamide) in nature were prepared.

To prepare specimens for ULAM processing discs of $\sim$10 mm diameter were punched from a coated aluminium panel, alternatively steel (and aluminium) substrate samples were cut from panels using a guillotine to give specimens $\sim$100 mm^2. To ensure that any burrs or asperities formed at the rear of the sample by the cutting process were removed, the rear of the specimen was polished using a silicon-carbide abrasive paper (Struers, Glasgow, UK). At all times great care was taken to insure the procedures used to cut the specimen from the sample panel and to prepare the specimen for ULAM processing resulted in the specimen remaining flat.

2.2. Ultra-low-angle microtomy

A schematic of the ULAM apparatus as employed in the production of ultra-low-angle tapers is presented in Fig. 1. The ULAM processing of samples was carried out on a Microm HM355S motorised rotary microtome (Optech Scientific Instruments, Thame, UK) equipped with a standard specimen clamp and a tungsten carbide knife. The ultra-low-angle sectioning blocks ($\sim$1230 mm^2 $\times$ 7 mm) were manufactured in-house from stainless steel. The ultra-low-angle sectioning blocks have one 1230 mm^2 tapered face raised by a defined amount (in μm) relative to the parallel edge of the tapered face. The ultra-low-angle sectioning blocks

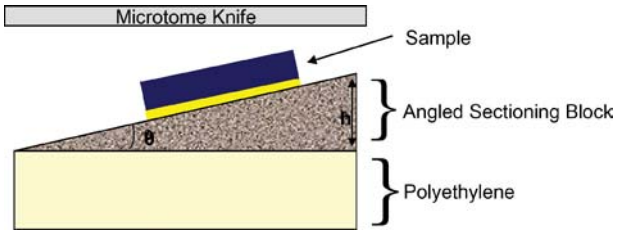

Figure 1 Schematic depicting the concept of ultra-low-angle microtomy operation.

available in our laboratories have tapered faces raised by a height of 25, 50, 100 and 200 μm (parameter h in Fig. 1), providing taper angles (θ in Fig. 1) of 0.04°, 0.08°, 0.16° and 0.33° respectively.

The following procedure was followed when processing coating samples by the ULAM technique:

(1) A polyethylene (PE) block (~160 × 160 × 20 mm) (Aquarius Plastics, Guildford, UK) was placed in the microtome sample clamp and trimmed with the tungsten-carbide knife until the sections comprised the complete face of the PE block. The PE block was then retracted from the knife and double-sided adhesive tape applied to the freshly trimmed PE block face.

(2) The face of an angled sectioning block containing an ultra-low-angle taper was cleaned with acetone (Fisher Scientific, Loughbrorough, UK) to insure it was free of any contaminants. Double sided adhesive tape was then applied to the taper containing face of the angled sectioning block and the specimen to be processed was applied to the adhesive tape at the centre of the angled sectioning block face.

(3) The angled sectioning block was then secured to the PE block via the double sided adhesive tape on the trimmed face of the PE block such that the specimen to be processed was presented to the microtome knife at an ultra-low-angle (see Fig. 1).

(4) The specimen was then sectioned at between 1 and 5 μm sectioning depth depending on the thickness of the sample coating. Once the desired interface was revealed or the required depth of tapering obtained the sample was removed from the angled sectioning block for analysis.

2.3. Scanning electron microscopy

SEM images were acquired on a Hitachi S3200N environmental SEM operated at a chamber pressure of 50 Pa. A 20 kV electron beam was employed for scanning to minimise any possible charging effects.

2.4. Atomic force microscopy

AFM images were acquired on a Digital Instruments Nanoscope III (California, USA) operated in the tapping mode. Tapered coating samples were fixed to metal AFM stubs prior to analysis. Ultrasharp Si NSCS11 cantilevers from NT-MDT (Moscow, Russia) were employed.

2.5. X-ray photoelectron spectroscopy

XPS analyses were performed on a Thermo VG Scientific Sigma Probe spectrometer (Thermo VG Scientific, East Grinstead, UK). The instrument employs a monochromated Al K_α X-ray source ($h\nu = 1486.6$ eV) which was used at 300 W (15 kV × 20 mA). The area of analysis was approximately 15 μm diameter for the PVdF/polyurethane interface sample. The pass energy was set at 20 eV for high-resolution spectra of all elements of interest. Charge compensation was achieved using an electron flood gun.

To aid charge compensation during linescan analysis on the PVdF/PU interface specimens the linear edge of a Mo grid was positioned such that it was at right angles to the interface region to be analysed. The Mo grid was held in place by a sprung Cu/Be clip which was also positioned so as to be at right angle to the interface region to be analysed. Experience has shown that this combination of Mo grid and Cu/Be clip geometry promotes stable charge compensation across the interface region to be investigated.

3. Results and discussion

3.1. Ultra-low-angle microtomy

In a previous paper it was demonstrated that the ultra-low-angle tapers produced from multilayer, polymeric coating systems by ULAM had application in both 'buried' interface analysis and compositional depth profiling by small area X-ray photoelectron spectroscopy [13]. However, before the ULAM technique can be accepted for general use two crucial uncertainties need to be resolved. Firstly, what is the state of the polymeric material along the taper after ULAM processing, specifically is any roughening or damage of the material surface observed? Secondly, how well-defined is the interface between the coating layers exposed by ULAM processing and is there any evidence of smearing of the polymeric material by the passage of the microtome knife?

The concept behind ULAM is very simple; a specimen is presented to the microtome knife at an ultra-low-angle (see Fig. 1) such that sectioning of the specimen by the microtome knife imparts an ultra-low-angle taper through the sample material. To demonstrate the applicability of ULAM to the investigation of organic materials a blue PVdF based topcoat formulation and a yellow PU based primer formulation were employed as a model, multilayer, polymeric coating system. In Fig. 2 a digitally recorded optical image of a PVdF/PU coating on Al substrate processed by ULAM such that the interface between the two coatings has been exposed is presented. The ultra-low-angle taper imparted by ULAM cuts the air/coating surface of the PVdF topcoat, traverses the bulk of the PVdF topcoat, exposes the PVdF/PU interface region and terminates in the PU primer bulk (as indicated by the arrow in Fig. 2). The image in Fig. 2 clearly demonstrates that ULAM is capable of exposing a 'buried' interface; in this case the interface is buried below 20 μm or more of the PVdF topcoat.

3.2. Morphology and topology of tapered polymeric surfaces

In Fig. 3a an SEM image of a region of the PVdF topcoat bulk exposed by ULAM processing is presented.

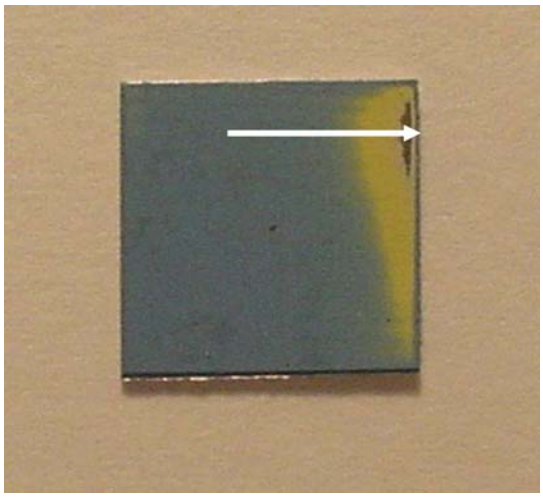

Figure 2 A digitally recorded optical image of a PVdF/poly(urethane) multilayer coating interface exposed by ultra-low-angle microtomy. The blue region is the PVdF based topcoat whilst the yellow region is the polyurethane based primer. The arrow indicates the direction followed by the ultra-low-angle taper imparted by ULAM processing.

The PVdF bulk exposed at the tapered surface in Fig. 3a exhibits two distinct morphologies. One of the morphological regions is flat and exhibits a low pixel intensity (dark contrast) in the SEM image. These regions of low pixel intensity are attributed to regions composed principally of the PVdF polymer resin. The alternate morphological region of the PVdF taper is granular in nature (the granules are $\sim$1 μm in diameter), a large number of the granules observed in Fig. 3a are associated with a very high pixel intensity (light contrast). The granules that exhibit a high pixel intensity are attributed to the presence of pigments in the PVdF coating formulation. In Fig. 4a a 400 μm^2 AFM tapping mode image of a region of the PVdF topcoat bulk exposed by ULAM processing, complementary to the SEM image of Fig. 3a, is presented. In Fig. 4a the PVdF tapered surface topography reveals the presence of a large number of polypoid structures, typically 2 μm in diameter. Such polypoid structures have been observed before for both AFM [14] and SEM [15] characterisation of pristine PVdF film surfaces. However, it is not possible to categorically assign the polypoid structures observed in Fig. 4a to PVdF alone, a number of the polypoid structures may be associated with the high pixel intensity granules observed in Fig. 3a. Surface roughness calculations for the AFM image in Fig. 4a give $R_a = 47 \pm 9$ nm (4 μm^2 area) suggesting the surface is relatively flat for one that has been sectioned by a microtome knife. However, this R_a value is much higher than would be expected for a pristine PVdF film where R_a values $<$5 nm have been reported [16]. No evidence is observed in Fig. 3a or 4a of any surface damage or roughening, suggesting that the microtome knife has cleaved the PVdF coating with minimal perturbation of the polymeric material.

In Fig. 3b an SEM image of a region of the PU primer bulk exposed by ULAM tapering is presented. It is observed that the morphology exhibited by the tapered PU surface in Fig. 3b contrasts markedly with that observed for the PVdF region in Fig. 3a. In a manner similar to the PVdF topcoat the PU primer possesses

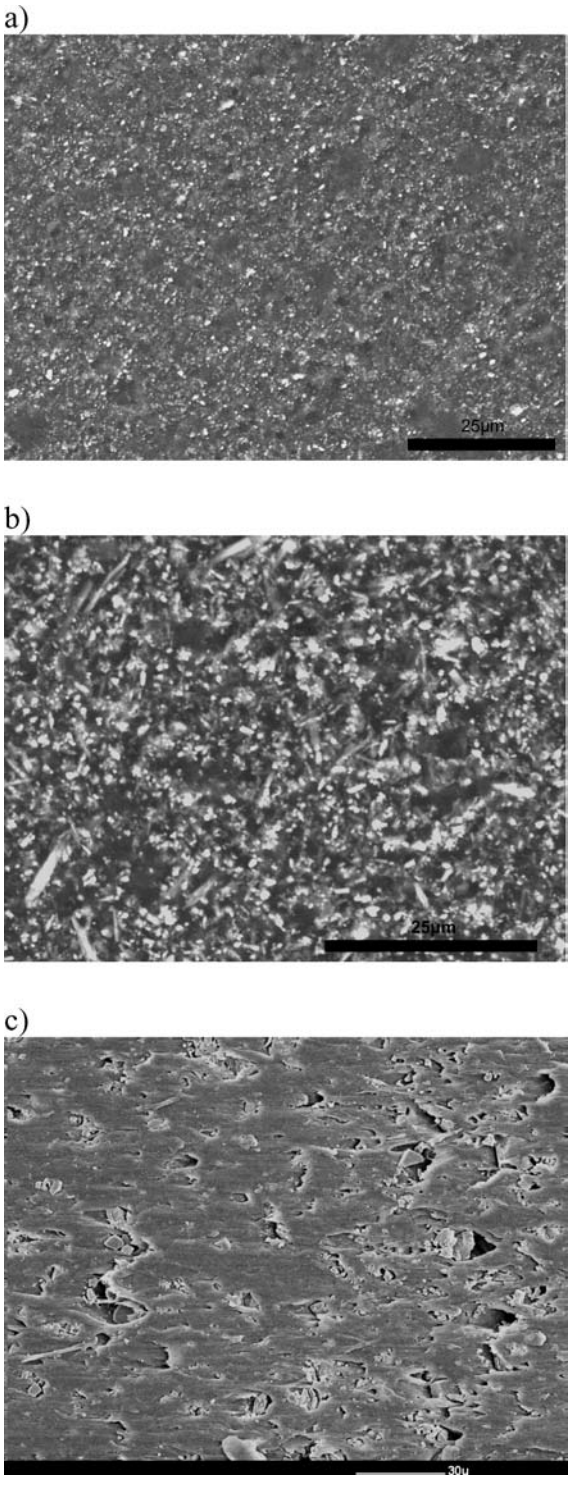

Figure 3 SEM images of polymer coating bulk acquired on tapers produced by ultra-low-angle microtomy: (a) PVdF bulk, (b) polyurethane bulk, and (c) polyamide/organosilane bulk.

regions of low pixel intensity (dark contrast) and regions that are granular and which exhibit higher pixel intensity (light contrast). These regions are attributed to PU polymer rich and pigment rich regions respectively. However, the PU surface morphology observed in Fig. 3b also exhibits a large number of needle or acicular structures at or protruding from the material surface. It is noted that these acicular structures are associated with a very high pixel intensity (very light contrast) in the SEM image. The observation of the acicular structures in Fig. 3b is attributed to the presence

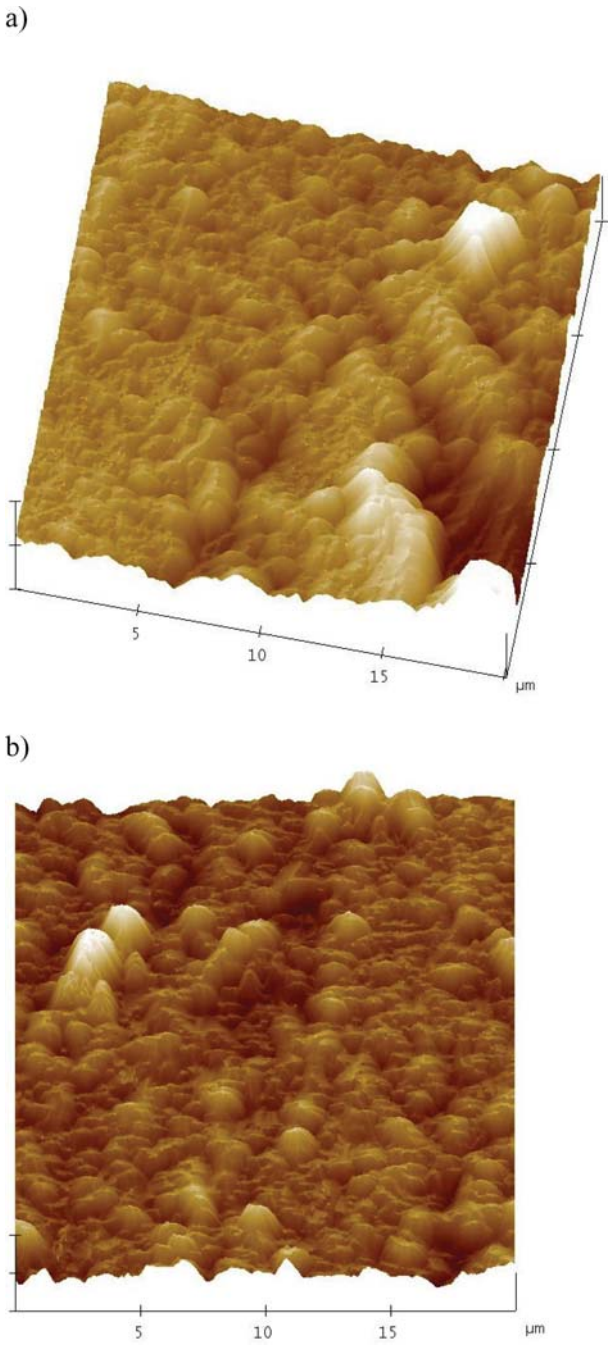

Figure 4 Atomic force microscopy tapping mode images, 400 μm^2, of (a) the poly(vinylidene difluoride) region and (b) the poly(urethane) region of a ULAM tapered PVdF/PU sample.

of strontium-chromate, in the PU coating. In Fig. 4b a 400 μm^2 AFM tapping mode image of the PU primer bulk, complementary to the SEM image in Fig. 3b, is presented. In Fig. 4b the topography of the PU surface is similar to that observed for the PVdF bulk region in Fig. 4a. However, the polypoid containing topography observed in Fig. 4b suggests that in the PU the polypoid structures are more discrete and many stand proud of or protrude from the sample surface. It is suggested that the polypoid structures standing proud or protruding from the sample surface are in fact the acicular structures observed in Fig. 3b. This would correlate with the fact that both titanium dioxide and barium sulphate, also used in the primer, have primary particle sizes of around 0.3 μm, much smaller than the primary particle size of the strontium chromate (12–14 μm). Calculations of surface roughness obtained from the AFM image in Fig. 4b give $R_a = 51 \pm 8$ nm (4 μm^2 area) indicating the surface is flat for one that has been sectioned by a microtome knife. However, this R_a value is much higher than would be expected for a pristine PU film where R_a values <2 nm (4 μm^2 area) have been reported [17]. As with the PVdF bulk region, no evidence is observed in Fig. 3b or 4b to indicate any damage to or roughening of the sample surface by tearing or stripping of the polymeric material.

In contrast to the well-ordered sample surfaces observed in Fig. 3a and b the SEM image in Fig. 3c displays large-scale surface damage leading to considerable surface roughening due to the tearing and stripping of the polymeric material. The SEM image in Fig. 3c was acquired on a poorly mounted polyamide/organosilane (PA) coating that was sectioned with a blunted knife. The damage observed on the PA coating is directional (that is the damage occurs in a left to right direction in the SEM image), this direction is consistent with that of the microtome knife as it passed through the polymeric material. It is also observed in Fig. 3c that some debris associated with the damage to the PA surface is still resident on the ULAM taper.

3.3. Morphology of buried interface exposed by ULAM

In Fig. 5a a low resolution SEM image of an interface region between a PVdF based topcoat (low pixel intensity/dark contrast region in Fig. 5a) and the underlying PU based primer (higher pixel intensity/light contrast region of Fig. 5a) is presented. The SEM image in Fig. 5a was acquired on a punched disk sample which upon ULAM processing commonly produces the curved interface region between the coatings that is observed in Fig. 5a. The interface region in Fig. 5a, even at low magnification, is well-defined and exhibits good resolution between the two coating layers. Further examination of Fig. 5a suggests there is no large scale evidence of smearing of the polymeric coatings indicating the microtome knife cleaves the coating across the interface in a precise manner. In contrast to the well-resolved interface region observed in Fig. 5a the PVdF/PU interface presented in Fig. 5b is poorly defined. The specimen used to obtain the SEM image in Fig. 5b was prepared from the same sample panel as the specimen used to obtain the SEM image in Fig. 5a. However, the specimen used in Fig. 5b was sectioned using a blunted and damaged microtome knife. In the author's opinion, the poorly defined PVdF/PU interface and the features observed at the interface in Fig. 5b result from localised damage to the cutting edge of the microtome knife. The use of such a knife has resulted in a poorly resolved interface and in the smearing of PVdF topcoat material across the PVdF/PU interface region into the PU bulk region of the specimen. In practice, the use of a sharp, pristine microtome knife is essential in ensuring that the exposed 'buried' interface exhibits a well-resolved and well-defined boundary between the two coating layers.

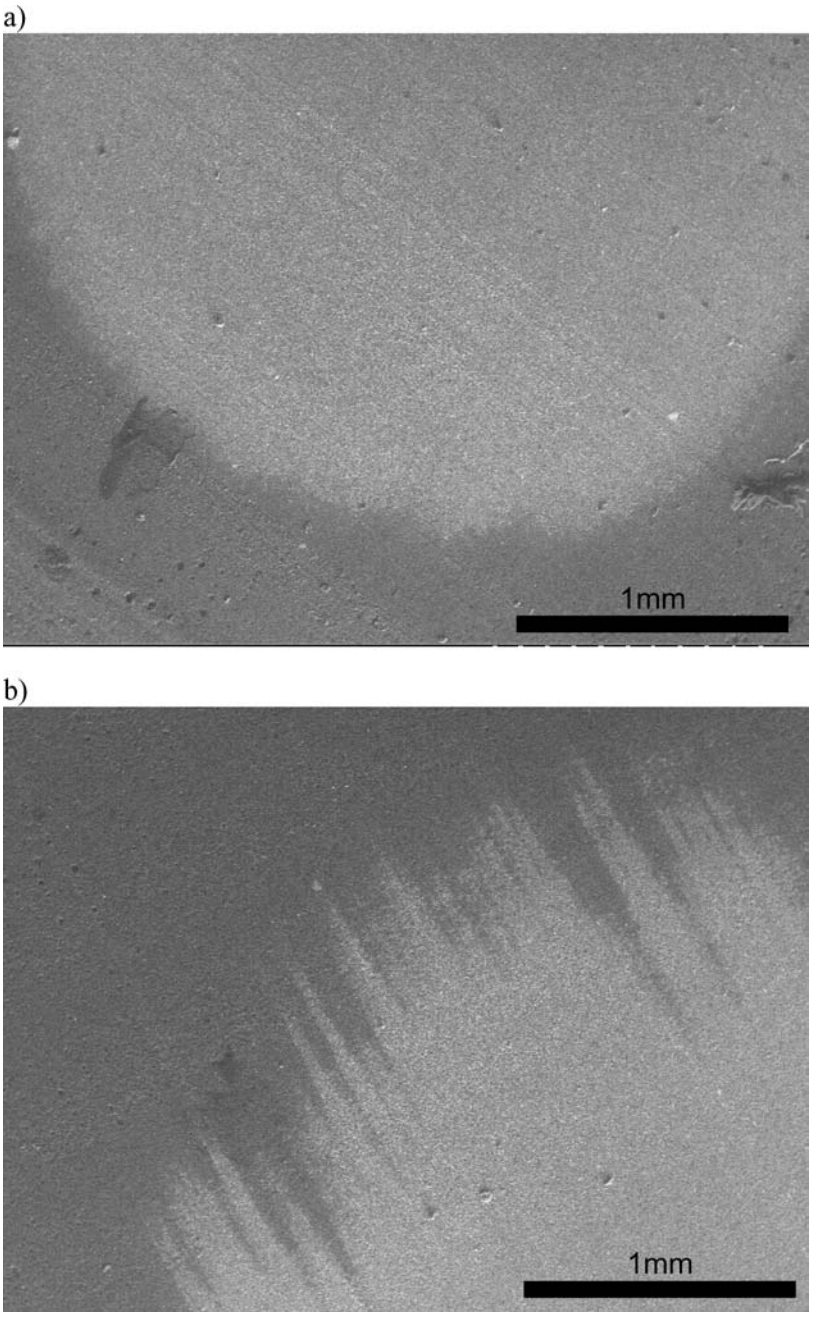

Figure 5 SEM low resolution images of the PVdF/polyurethane interface exposed by ultra-low-angle microtomy: (a) PVdF/polyurethane interface exposed by a sharp microtome knife and (b) PVdF/polyurethane interface exposed by a blunted and pitted microtome knife.

In the discussion above regarding the characterisation of the PVdF and PU surface morphologies and topologies resulting from ULAM processing it was noted that the two coating formulations exhibit markedly different morphologies and at a qualitative level differences in SEM pixel intensity. These differences in morphology and pixel intensity allow us to readily distinguish the PVdF from the PU across the PVdF/PU interface observed in Fig. 6. To aid identification of the PVdF/polyurethane interface broken lines indicating the locus of the interface have been inserted into the SEM images in Fig. 6a and b. In both Fig. 6a and b the low contrast/pixel intensity region to the left of the PVdF/PU interface is the PVdF topcoat whilst the higher contrast/pixel intensity region to the right of the interface is the PU primer. The SEM images of the PVdF/PU interface in Fig. 6 were acquired at higher resolution than those obtained in Fig. 5. The SEM image in Fig. 6a was acquired at $\times 350$ magnification while that in Fig. 6b was acquired at $\times 800$ magnification. The SEM images in Fig. 6a and b demonstrate that the PVdF/PU interface is well-defined and that the two coatings are distinct and readily resolved across the exposed interface. The higher resolution images in Fig. 6 support the assertion that there is no apparent evidence of smearing of the two polymeric coatings upon cleavage by the microtome knife.

3.4. XPS linescan analysis of a 'buried' PVdF/PU interface

ULAM has been applied to the investigation, by XPS linescan, of changes in the elemental concentration (at.%) with depth across the interface between a PVdF

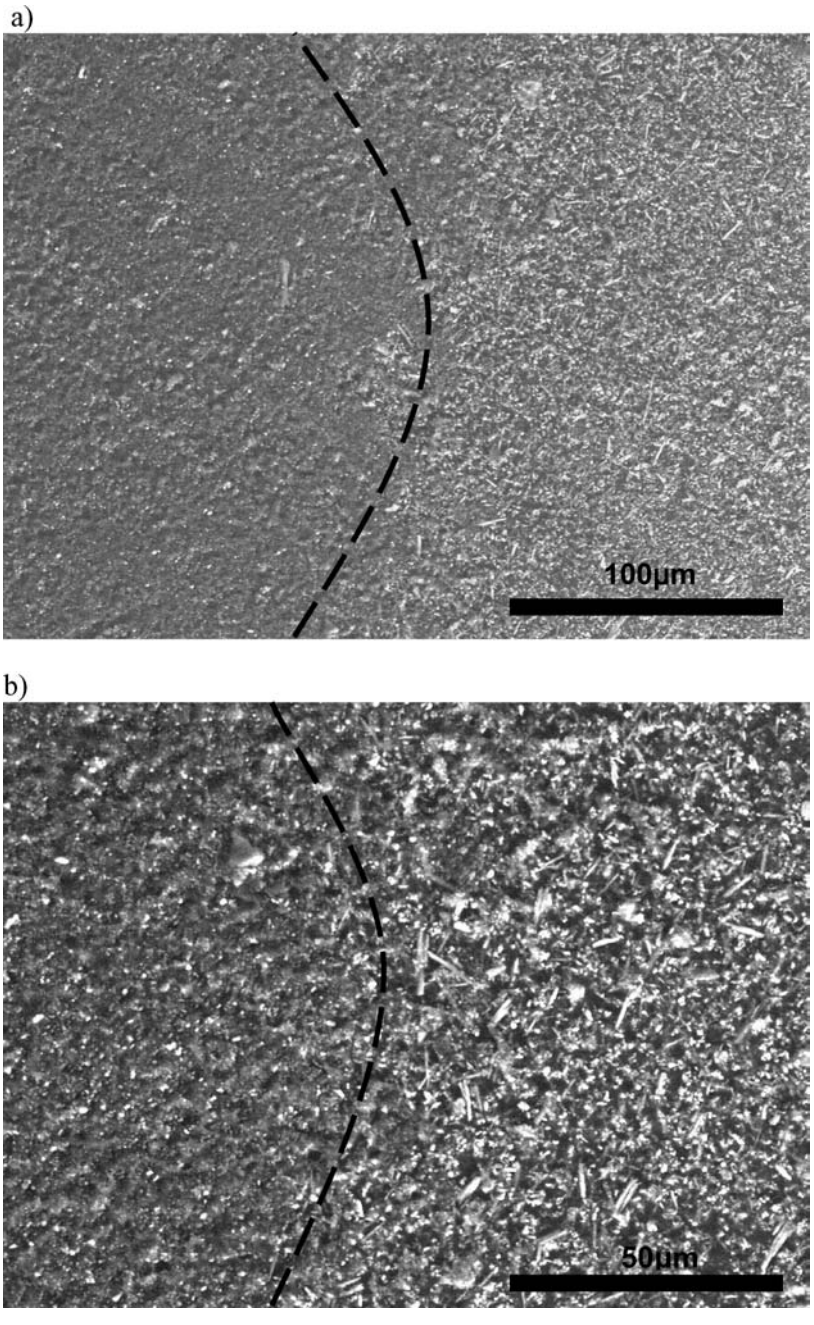

Figure 6 SEM images of the PVdF/polyurethane interface exposed by ultra-low-angle microtomy: (a) PVdF/polyurethane interface and (b) the same interface at higher resolution. The broken lines indicate the locus of the interface between the PVdF topcoat and the polyurethane primer.

topcoat and a PU primer. Before considering this interface, which has been 'buried' 20–25 μm below the air/coating surface of the PVdF topcoat, it is instructive to dwell on the results from the analysis of the bulk sections of both coatings. The concentration of the fluorine is around 15% whereas a typical surface concentration in a 70:30 blend of PVdF and acrylic resins is close to 30% demonstrating the segregation of fluorine containing moieties to the air/coating surface probably as a result of the natural tendency to reduce surface free energy.

The commercially based formulations chosen for this analysis are known to provide a strong adhesion between the PVdF based topcoat and the underlying PU based primer. Changes in the elemental concentration with respect to depth of all the major constituent elements of the coatings have been followed, the results of which are presented in Fig. 7. However, minor constituents with concentrations <0.3% (primarily Sr, Cr and Ba found in the PU primer) have been omitted from Fig. 7. for reasons of clarity. The initial data obtained from a linescan along a ULAM taper across a coating/coating interface is that of atomic composition (at.%) with horizontal distance. However, with knowledge of the ULAM angle and XPS linescan step size employed, application of simple geometry (Equation 1 below) readily enables the horizontal distance to be transformed into a depth interval and a chart describing elemental concentration with depth is readily constructed as is demonstrated in Fig. 7.

$$\Delta z = b \tan \theta \tag{1}$$

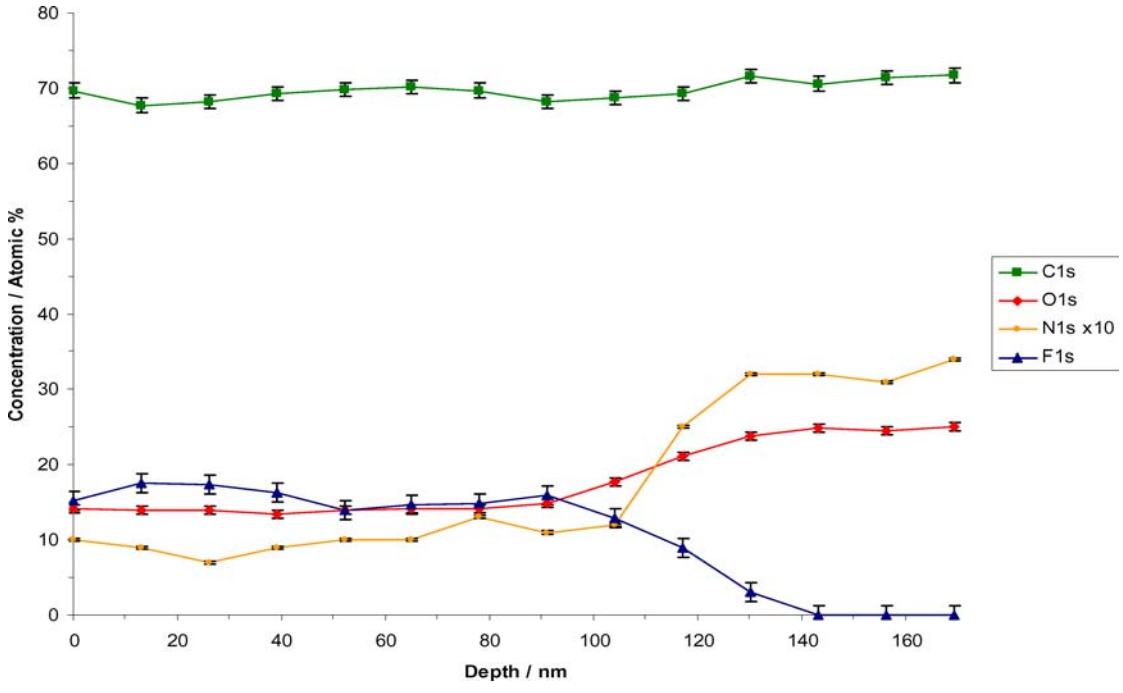

Figure 7 Changes in C, O, F and N concentration traversing a ULAM produced taper exposing a 'buried' PVdF/PU interface region. The taper was cut using a 0.04° angle, a 15 μm X-ray spot size and a 18 μm linescan step size were employed, thus, theoretically, each successive analysis point increases the analysed depth by 13 nm. The values of the N1s data series have been multiplied by a factor of 10 for reasons of clarity.

where Δz = depth resolution, b = XPS linescan step size, θ = ULAM taper angle. For the linescan analysis described here the sample was sectioned using the 0.04° taper angle (θ), a 15 μm X-ray spot and a 18 μm XPS linescan step size (b) were employed giving a theoretical depth resolution (Δz) of 13 nm.

In Fig. 7 the results obtained from an XPS linescan analysis detailing changes in the concentration of C, O, F and N with respect to analysed depth across a buried PVdF/PU interface are presented. The initial point of analysis in Fig. 7 (depth 0 nm) is within the PVdF bulk whilst the final analysis point (depth 169 nm) lies within the PU bulk. It is observed in Fig. 7 that the interface region varies for the different elements. The interface as defined by fluorine starts at 91 nm and ends at 143 nm a distance of 52 nm. The oxygen interface begins and ends in the same place but the nitrogen interface only starts at 103 nm and ends at 130 nm and the carbon interface is even narrower beginning at 110 nm and finishing at 130 nm. Thus, elemental concentration changes attributed to the PVdF/PU interface are observed over depths between 20–50 nm. The data for C in Fig. 7 indicates that there is a small change in the concentration of C as the analysis traverses the PVdF/PU interface. In the PVdF bulk region of the taper (0–91 nm depth) the concentration of C is ∼69% this increases across the interface region to ∼71% in the PU bulk region (130–169 nm) of the analysis. These depth profile concentration values for the bulk regions of the coatings for C are consistent with XPS reference spectra obtained for the bulk of each coating formulation. Due to the small differences it is difficult to infer anything significant in this case. The concentration of F is ∼16% in the PVdF bulk; it is observed in Fig. 7 that the concentration of F gradually decreases across the PVdF/PU interface region (91–130 nm) as the ULAM taper results in the thinning of the PVdF topcoat. No signal for F is observed beyond 143 nm (the PU region of the taper sample). The decrease in the concentration of F is countered by increases in the concentrations of O and N as observed in Fig. 7. In the PVdF bulk region of the taper the concentrations of O and N are ∼14% and ∼1% respectively. The concentration of O and N increase across the PVdF/PU interface to reach concentration levels of ∼24% for O and ∼3.2% for N within the PU bulk. The analysis point at a depth of 130 nm suggests there has been some diffusion of F bearing materials from the PVdF topcoat into the topmost nanometres of the underlying PU primer [13]. At this analysis point the N concentration (∼3.25 at%) has reached a level consistent with the N signal arising from the PU bulk; however a residual F signal (∼3%) is still observed. This penetration of the PVdF topcoat into the PU primer may result in the strong adhesion these coating formulations exhibit towards each other. The oxygen curve demonstrates the opposite effect and indicates that the oxygen rich species migrate into the PVdF topcoat thereby widening the interfacial region with the consequence of further improvement in the interfacial adhesion.

According to geometrical considerations a step change interface can be identified to within a band 13 nm wide. This broadening is a natural consequence of the size of the small area XPS X-ray spot and its transformation to a depth on the ULAM section. In practice an interfacial region is defined as the distance over which the concentration of an element reduces from 84% of its maximum intensity to 16% of that intensity. That is, one standard deviation either side of the step change position. Thus the interfacial region is described by the limits 16 and 84% of the change. This is the usual manner in which interface width, Δz, is defined in compositional depth profiles obtained by surface

analysis methods. By consideration of the carbon profile obtained in this work, which will not be greatly affected by interdiffusion of PVdF and PU (which is at a low level), the depth resolution is estimated at 25 nm. The fact that the depth profiles for carbon, oxygen, nitrogen and fluorine in Fig. 7 do not follow each other in a "mirror like" manner across the interface taken together with the above hypothesis indicates that the results showing inter-diffusion of fluorine and oxygen containing moieties in different directions across the interface are highlighting a real effect.

4. Conclusions

We have demonstrated by use of a PVdF and PU based model, multilayer, polymeric coating system that the tapered sample surface, produced by ULAM processing, exhibits no surface damage or roughening as a result of sectioning with a microtome knife. Evidence for surface damage and roughening on a polyamide/organosilane taper surface resulting from incorrect mounting practices and sectioning with a blunted microtome knife was also demonstrated. Analysis of a PVdF/PU interface 'buried' more the 20 μm below the PVdF topcoat revealed a well-defined and well-resolved interface region had been exposed by ULAM processing. No evidence of sample smearing across the PVdF/PU interface was observed in samples sectioned with a sharp microtome knife. However, it was demonstrated that samples sectioned with a blunted and damaged microtome knife possessed poorly resolved interfaces which also exhibited evidence of polymer smearing. We have also demonstrated by XPS linescan the applicability of ULAM tapers to compositional depth profiling and the investigation of 'buried' interfaces. Changes in the elemental concentration of C, O, F and N across a model, multilayer PVdF/PU coating interface were described. Additionally, the XPS analysis indicated penetration of F bearing components from the PVdF topcoat into the underlying PU primer. In general, ULAM is readily capable of producing sample tapers with well-defined geometries and of exposing 'buried' interfaces that are well resolved. Although in the studies reported here we have restricted ULAM processing to polymeric coating materials the technique may be more generally applied to any material system compatible with being sectioned by a microtome knife.

Acknowledgements

The authors gratefully thank Ms Marianne Guichenuy for use of the polyamide/organosilane SEM image, Dr Peter Zhdan for assistance with AFM image acquisition and Mr Andy Brown for assistance with SEM image acquisition. The authors acknowledge the financial support of the EPSRC (Grant no. GR/N65745).

References

1. P. J. CUMPSON, *J. Electr. Spectr. Relat. Phenom.* **73** (1995); C. PERRUCHOT, J. F. WATTS, C. LOWE, R. G. WHITE, and P. J. CUMPSON, *Surf. Interf. Anal.* **33** (2002) 10.
2. G. J. ROSS, N. P. BARRADAS, M. P. HILL, C. JEYNES, P. MORRISSEY and J. F. WATTS, *J. Mater. Sci.* **36** (2001) 4731.
3. S. GIROIS, L. AUDOUIN, J. VERDU, P. DELPRAT and G. MAROT, *Polym. Degrad. Stab.* **51** (1996) 125.
4. C. ANTON-PRINET, J. DUBOIS, G. MUR, M. GAY, L. AUDOUIN and J. VERDU, *ibid.* **60** (1996) 125.
5. K. ADAMSON, *Prog. Org. Coat.* **45** (2002) 69.
6. J. M. WALLS, D. D. HALL and D. E. SYKES, *Surf. Interf. Anal.* **1** (1979) 204.
7. J. M. WALLS, *Thin Solid Films* **80** (1981) 213.
8. M. L. TARNG and D. G. FISHER, *J. Vac. Sci. Technol.* **15** (1978) 50.
9. H. E. HINTERMANN and L. CHOLLET, *Surf. Techn.* **8** (1979) 421.
10. C. LEA and M. P. SEAH, *Thin Solid Films* **75** (1981) 67.
11. J. M. COHEN and J. E. CASTLE, *Inst. Phys. Conf. Ser.* No **93** (1988) Chapt. 5 275.
12. M. GUICHENUY, J. F. WATTS, M.-L. ABEL, A. M. BROWN, M. AUDENAERT and N. AMOUROUX, Accepted for publication in *Surf. Interf. Anal.* Aug. 2004.
13. S. J. HINDER, J. F. WATTS and C. LOWE, Accepted for publication in *Surf. Interf. Anal.* Aug. 2004.
14. M. C. PORTE-DURRIEU, C. AYMES-CHODUR, C. VERGNE, N. BETZ and C. BAQUEY, *Nucl. Instr. Meth. Phys. Res. B* **151** (1999) 404.
15. N. CHEN and L. HONG, *Polymer* **43** (2002) 1429.
16. M. D. DUCA, C. L. PLOSCEANU and T. POP, *Polym. Degrad. Stab.* **61** (1998) 65.
17. T.-W. CHUNG, D.-Z. LIU, S.-Y. WANG and S.-S. WANG, *Biomaterials* **24** (2003) 4655.

Received 23 March
and accepted 20 August 2004